Biomaterials 101 (2016) 217–228

Contents lists available at ScienceDirect

Biomaterials

journal homepage: www.elsevier.com/locate/biomaterials

Mechanically resilient, injectable, and bioadhesive supramolecular gelatin hydrogels crosslinked by weak host-guest interactions assist cell infiltration and in situ tissue regeneration

Qian Feng [a, b, 1], Kongchang Wei [a, b, c, 1], Sien Lin [a, g], Zhen Xu [h], Yuxin Sun [g], Peng Shi [h], Gang Li [g], Liming Bian [a, c, d, e, f, *]

[a] Division of Biomedical Engineering, The Chinese University of Hong Kong, Shatin, New Territories 999077, Hong Kong
[b] Department of Mechanical and Automation Engineering, The Chinese University of Hong Kong, Shatin, New Territories 999077, Hong Kong
[c] Shun Hing Institute of Advanced Engineering, The Chinese University of Hong Kong, Shatin, New Territories 999077, Hong Kong
[d] Shenzhen Research Institue, The Chinese University of Hong Kong, Hong Kong
[e] China Orthopedic Regenerative Medicine Group (CORMed), Hangzhou, China
[f] Centre of Novel Biomaterials, The Chinese University of Hong Kong, Hong Kong
[g] Department of Orthopaedic and Traumatology, The Chinese University of Hong Kong, Prince of Wales Hospital, New Territories 999077, Hong Kong
[h] Department of Mechanical and Biomedical Engineering, City University of Hong Kong, Tat Chee Avenue, Kowloon 999077, Hong Kong

ARTICLE INFO

Article history:
Received 8 March 2016
Received in revised form
9 May 2016
Accepted 24 May 2016
Available online 2 June 2016

Keywords:
Supramolecular hydrogel
Host-guest complexation
Biomaterial carrier
Drug delivery
Tissue regeneration

ABSTRACT

Although considered promising materials for assisting organ regeneration, few hydrogels meet the stringent requirements of clinical translation on the preparation, application, mechanical property, bioadhesion, and biocompatibility of the hydrogels. Herein, we describe a facile supramolecular approach for preparing gelatin hydrogels with a wide array of desirable properties. Briefly, we first prepare a supramolecular gelatin macromer via the efficient host-guest complexation between the aromatic residues of gelatin and free diffusing photo-crosslinkable acrylated β-cyclodextrin (β-CD) monomers. The subsequent crosslinking of the macromers produces highly resilient supramolecular gelatin hydrogels that are solely crosslinked by the weak host-guest interactions between the gelatinous aromatic residues and β-cyclodextrin (β-CD). The obtained hydrogels are capable of sustaining excessive compressive and tensile strain, and they are capable of quick self healing after mechanical disruption. These hydrogels can be injected in the gelation state through surgical needles and re-molded to the targeted geometries while protecting the encapsulated cells. Moreover, the weak host-guest crosslinking likely facilitate the infiltration and migration of cells into the hydrogels. The excess β-CDs in the hydrogels enable the hydrogel-tissue adhesion and enhance the loading and sustained delivery of hydrophobic drugs. The cell and animal studies show that such hydrogels support cell recruitment, differentiation, and bone regeneration, making them promising carrier biomaterials of therapeutic cells and drugs via minimally invasive procedures.

1. Introduction

Among many biomaterials developed for applications in regenerative medicine, hydrogels have received increasing attention due to their similarity to biological tissues in terms of their high water content, tunable physical and biological properties [1–9]. Up to date, great success has been achieved in using hydrogels to emulate stem cell microenvironments for controlling stem cell differentiation and tissue regeneration [10–13]. A number of hydrogels for both *in vitro* and *in vivo* studies have been developed in order to reveal fundamental understanding of cell-material interactions and their roles in directing tissue regeneration [14–16]. However, it is still challenging to prepare hydrogels that can simultaneously fulfill the stringent requirements for real applications in tissue engineering. Such requirement usually include

* Corresponding author. Division of Biomedical Engineering, The Chinese University of Hong Kong, Shatin, New Territories 999077, Hong Kong.
E-mail address: lbian@mae.cuhk.edu.hk (L. Bian).
[1] Theses authors contributed equally.

http://dx.doi.org/10.1016/j.biomaterials.2016.05.043
0142-9612/

facile preparation, easy surgical application, robust mechanical properties, tissue adhesion, excellent biocompatibility and bioactivity, etc [17–22]. Herein, we describe the facile preparation of supramolecularly engineered gelatin hydrogels that can meet such challenging requirements in real applications.

Gelatin has been extensively used to fabricate hydrogels for tissue engineering, due to its good biocompatibility, intrinsic bioactivity and abundancy [23–26]. However, chemical crosslinking is often necessary to stabilize gelatin hydrogels, because the native gelatin hydrogels spontaneously formed at low temperatures (<30 °C) are not stable under the physiological conditions [27]. The physical crosslinking of gelatin triple helix will be disrupted at temperatures above 30 °C [28]. Therefore, to prepare stable hydrogels for biomedical applications, gelatin is usually chemically functionalized by polymerizable groups, yielding the crosslinkable gelatin macromers such as the methacrylated gelatin (MeGel) [29–31]. Subsequent crosslinking of such macromers produces stable gelatin hydrogels that have been used in many cell studies [32]. However, most of these chemically crosslinked gelatin hydrogels are brittle and hard for post-gelation processing, thus precluding it from widespread surgical applications [33]. For example, the MeGel hydrogels fails at a low compressive or tensile strain and are not capable of self-healing, and this makes the MeGel hydrogels not suitable for application in load bearing sites such as joint cartilage. The inability to inject the MeGel hydrogels in the gelation state makes the use of the MeGel hydrogels in minimal invasive procedures difficult.

To address these challenges, we propose a novel "Host-Guest Macromer" approach to prepare mechanically robust gelatin hydrogels with desirable supramolecular properties and biological functions. Instead of the chemically functionalized gelatin macromer, the host-guest supramolecular macromer (HGM) is used as the hydrogel precursor. Free from chemical modifications of the biopolymers, the HGM is formed via the efficient host-guest complexation between aromatic residues of gelatin (e.g., phenylalanine, tyrosine, and tryptophan) and the free diffusing photocrosslinkable acrylated β-cyclodextrins (Ac-β-CDs). Subsequent UV-initiated polymerization of the Ac-β-CDs produces the mechanically robust hydrogels with gelatin polymers physically crosslinked by host-guest interactions (termed HGM hydrogel). Such supramolecularly engineered gelatin HGM hydrogels can form highly deformable and resilient 3D constructs under the physiological condition. They can be injected through 18G needles without compromising the viability of the encapsulated human mesenchymal stem cells (hMSCs) due to the reversible nature of the host-guest interactions. In addition, many hydrophobic small molecules such as dexamethasone and kartogenin are effective inducting agents of stem cell differentiation, which is important to the regeneration of the injured tissues [34,35]. However, these hydrophobic small molecules are difficult to be effectively loaded in the conventional hydrophic hydrogel network with a sustained long term release [36,37]. The excess β-CDs not only engender the adhesion of the hydrogels to biological tissues by the coupling to the aromatic groups of the native proteins and but also allow the delivery of hydrophobic drugs via the hydrophobic cavity. Furthermore, *in vitro* and *in vivo* studies show that such hydrogels support cell infiltration, differentiation and *in situ* bone regeneration, making them promising carriers of therapeutic cells and drugs via minimally invasive procedures. This simple but effective strategy opens up a new route to develop biopolymer-based supramolecular hydrogels with enhanced physical and biological functionalities as drug and/or cell carriers for regenerative medicine.

2. Materials and methods

2.1. Materials

β-cyclodextrin (β-CD), acrylate chloride and hydrogen peroxide (H_2O_2) were bought form Aladdin. Gelatin (type A, from porcine skin, isoelectric point: 7–9, Cat. No.: G1890-500G, Sigma), methacrylic anhydride, dimethylmalenic acid (DMMA), deuterium oxide (D_2O), dimethylsulfoxide-d6 (DMSO-d_6), dexamethasone (Dex), 2-hydroxy-4'-(2-hydroxyethoxy)-2-methylpropiophenone (I2959), 4′, 6-diamidino-2-phenylindole (DAPI), 3-(Trimethoxysily) propyl methacrylate, sliver nitrate, paraformaldehyde, Triton X-100, sodium thiosulfate, Triethyl amine (TEA), ethidium bromide, hyaluronidase were purchased from Sigma. Dimethyl Formamide (DMF), dimethylsulfoxide, acetone, hydrochloric acid (HCl), and sodium hydroxide (NaOH) were purchased from Fisher Scientific. Poly (ethylene glycol) diacrylate (PEGDA) were purchased from Jenkem. Phosphate buffered saline (DPBS), α-minimum essential medium (DMEM), penicillin, streptomycin, L-glutamine, calcein AM, fetal bovine serum (FBS), and Trizol were obtained from Gibco. BCA protein assay kit, calcium colorimetric assay kit, and revertAid First strand cDNA synthesis kit were obtained from Thermo. Peroxidase substrate kit DAB and vectastain ABC kit were purchased from Vector Lab. Human mesenchymal stem cells (hMSCs) from Lonza.

2.2. Synthesis of Acrylate β-cyclodextrin (Ac-β-CD)

10 g β-CD was added into 150 mL DMF with 7 mL TEA added into the solution. The mixture was stirred and cooled down to 0 °C before 5 ml acrylic acid was added into the solution. After stirring for 12 h, the mixture was filtrated to remove trimethylamine hydrochloride and the obtained clear solution was concentrated to about 20 ml by vacuum rotary evaporation. Then the solution was dripped into 600 ml acetone to precipitate the modified cyclodextrin. The precipitate was washed several times with acetone and vacuum dried for 3 days. The substitution degree (DS) of CD as 1 is confirmed by ^{1}H NMR (Bruker Advance 400 MHz spectrometer). It was recorded with DMSO-d_6 as the internal reference at 37 °C. In order to confirm the complexation between the Ac-β-CD and the benzene ring of gelatin, two dimensional nuclear overhauser effect spectroscopy (2D NOESY) was performed in D_2O with a Bruker Advance 400 MHz spectrometer at 37 °C.

2.3. Synthesis of methacrylated gelatin (MeGel)

10 g gelatin (type A) was dissolved in 100 mL PBS at 50 °C. A total of 12 mL methacrylic anhydride was then added to the 10% gelatin solution and stirred for 4 h at 50. The resulting mixture was dialyzed against DI water for one week at 45 °C to remove unreacted reagent (6 KDa cut-off dialysis membrane). Then, the liquid was lyophilized for 4 days at −104 °C. The degree of methacrylation as 3.17×10^{-4} mol per gram was determined by ^{1}H NMR (Bruker Advance 400 MHz spectrometer). It was recorded in D_2O with DMMA as the internal reference at 37 °C.

2.4. Preparation of hydrogels

2.4.1. HGM supramolecular gelatin hydrogel

Gelatin and Ac-β-CD was dissolved in PBS at 37 °C to produce mixture solutions with fixed concentration of gelatin (8% (w/v)) and varying amount of Ac-β-CD (0% (w/v), 4% (w/v) and 10% (w/v)). Then initiator I2959 was added at 0.05% (w/v). The mixture was pipetted into PVC molds at 37 °C, cooled down to 25 °C, and then exposed to 365 nm ultraviolet (UV) light (10 mW/cm^2, 10 min) at

25 °C to form supramolecular hydrogels with varying amount of Ac-β-CD, named Gel_xCD_y where, x and y represents the concentration (w/v%) of gelatin and Ac-β-CD, respectively.

2.4.2. MeGel hydrogel

8% (w/v) of methacrylated gelatin and 0.05% (w/v) of I2959 were dissolved in PBS at 37 °C. The solution was pipetted into PVC molds and cooled down to 25 °C before exposed to 365 nm UV light (10 mW/cm^2, 10 min) at 25 °C to obtain chemically crosslinked gelatin hydrogel, named MeGel.

For different test, PVC molds of different sizes were used.

2.5. Hydrogel swelling analysis

To evaluated the swelling, the freshly prepared MeGel and HGM hydrogels (200 μL per gel, n = 5) were incubated free floating at 37 °C in PBS for 24 h. Then, the samples were blotted to remove the residual surface liquid, and the swollen weight was recorded. Samples were than lyophilized and weighed once more to determine the dry weight of the hydrogels. The mass swelling ratio was then calculated as the ratio of swollen hydrogel mass to the mass of dry polymer.

2.6. Rheological measurement

Time sweep and shear thinning test were performed on an Anton Paar MCR301 rheometer with 25 mm diameter plates (plate to plate) at a 0.2 mm gap size. The hydrogels were homogeneously distributed between the top and bottom plates of the rheometer. Time sweeps were recorded at a strain of 0.1% and a frequency of 10 Hz. For shear thinning test, the sample underwent sequential shear with strain of 0.1% (for 120 s) and 1000% (for 60 s) for 4 cycles, and the recovery of storage (G′) and loss modulus (G″) were monitored by time sweeps at fixed frequency (10 Hz).

2.7. Tensile mechanical testing

Tension test were done on samples of 5 mm width × 2 mm thickness × 10 mm length (directly secured by the mechanical clamps) at an extension speed of 1 mm/s using a MACH-1 Micromechanical System. Tensile fatigue test was done with a tensile strain of 60% (at 25 °C) or 100% (at 37 °C) for 10 cycles (30 s for every cycle) at the same load speed.

For the tensile testing of the injected HGM hydrogels, pre-prepared HGM hydrogels (3 mm diameter × 4 mm thickness) were injected into the mold (5 mm width × 2 mm thickness × 10 mm length) and allowed to fully adapt to the shape of the mold for 3 min at 37 °C before testing. Then, the injected HGM hydrogels were secured by the mechanical clamps directly to conduct the tensile test at an extension speed of 1 mm/s.

2.8. Analysis of hMSCs migration in the hydrogels in vitro

Migration test was done by using the 24-well transwell. HGM and MeGel hydrogels were formed on the top of the transwell membrane, and the transwell setups were placed into a 24-well plate. The volume of each hydrogel was 30 μL. Then 100 μL medias of hMSCs (2×10^6/ml) were added on the top of the hydrogels, and 770 μL growth media with 10 ng/mL SDF-1 was added into the 24-well plates. After 2 h of incubation, the hydrogels were fixed by 4% paraformaldehyde and stained by DAPI. The confocal micrographs were obtained to visualize the distribution of the cells in the hydrogels.

2.9. Lap shear test of the hydrogel adhesive strength

50 μL of HGM or MeGel hydrogels were prepared between two overlapped glass slides (70 mm length × 26 mm width) with a 10 mm × 26 mm overlapping area. These two slides were pulled to the opposite direction at a rate of 2 mm/min until the failure of the hydrogels and separation of the two glass slides (MACH-1 Micromechanical System).

2.10. Analysis of the release of encapsulated dexamethasone from the hydrogels in vitro

HGM or MeGel hydrogels (n = 4) were photocrosslinked in 6 mm diameter × 3 mm thickness PVC molds. In order to wash off the excess I2959, hydrogels were soaked in 5 mL PBS for 6 h, and at every 2 h interval the PBS was changed. Then the hydrogels were transferred into 400 μL of 1 μM Dex solutions (in PBS) for 4 h. The Dex solutions were collected to test the absorbance at 242 nm. The percentage of Dex loaded into the hydrogels was calculated based on the standard curve.

The hydrogels obtained from the Dex loading experiments were incubated in 350 μL of PBS. PBS solution were collected and replenished at 6 h, 1 day, 3 day, 7 day, and 14 day. Measure the absorbance at 242 nm for these solutions to calculate the percentage of releasing Dex.

2.11. In vitro culture of hMSC-laden hydrogels

hMSCs were expanded to passage 4 by using growth medium consisting of α-minimum essential medium with 16.7% fetal bovine serum, 1% penicillin/streptomycin and 1% L-glutamine. For three-dimensional (3D) culture, 1% (w/v) poly (ethylene glycol) diacrylate (PEGDA) was added during the fabrication of the hMSC-laden HGM supramolecular gelatin hydrogels in order to prolong the stability of the HGM hydrogels for long term culture (n = 10 for each group). The addition of the PEGDA at this low concentration does not significantly alter the unique features of the HGM hydrogels as described above (Fig. S5c). PEGDA was only added for the fabrication of the HGM hydrogels used in the cell culture and animal experiments, and no PEGDA was added in the HGM hydrogels for all the other experiments. 1×10^7/mL hMSCs were then photoencapsulated with 365 nm UV (10 mW/cm^2, 5 min) into HGM or MeGel hydrogels. Osteogenic media (α-minimum essential medium with 16.7% fetal bovine serum, 1% penicillin/streptomycin, 1% L-glutamine, 10 mM β-glycerophosphate disodium, 50 μg/ml L-ascorbic acid 2-phosphate sesquimagnesium salt hydrate, and 100 nM Dexamethasone) were used for both 2D and 3D culture *in vitro*. The media were refreshed every 3 days during the *in vitro* culture. Viability was tested on 3D cell culture samples by calcein AM (Live) and ethidium bromide (Dead). For the *in vitro* culture of Dex loaded HGM hydrogels, we loaded 0.1 mM Dex and hMSCs into the HGM hydrogels simultaneously. Then, during the *in vitro* culture, the osteogenic media without Dex was used.

2.12. Subcutaneous implantation of hydrogels in nude mice

Four different groups of HGM hydrogels (n = 4 for each group) were implanted into the subcutaneous pockets on the backs of nude mice (4 pockets for every nude mouse). After 14 days of implantation, the harvested samples were fixed by 4% paraformaldehyde for analysis.

2.13. Rat calvarial defect repair with hydrogels

The male Sprague-Dawley albino rats (SD rats, 8 weeks old)

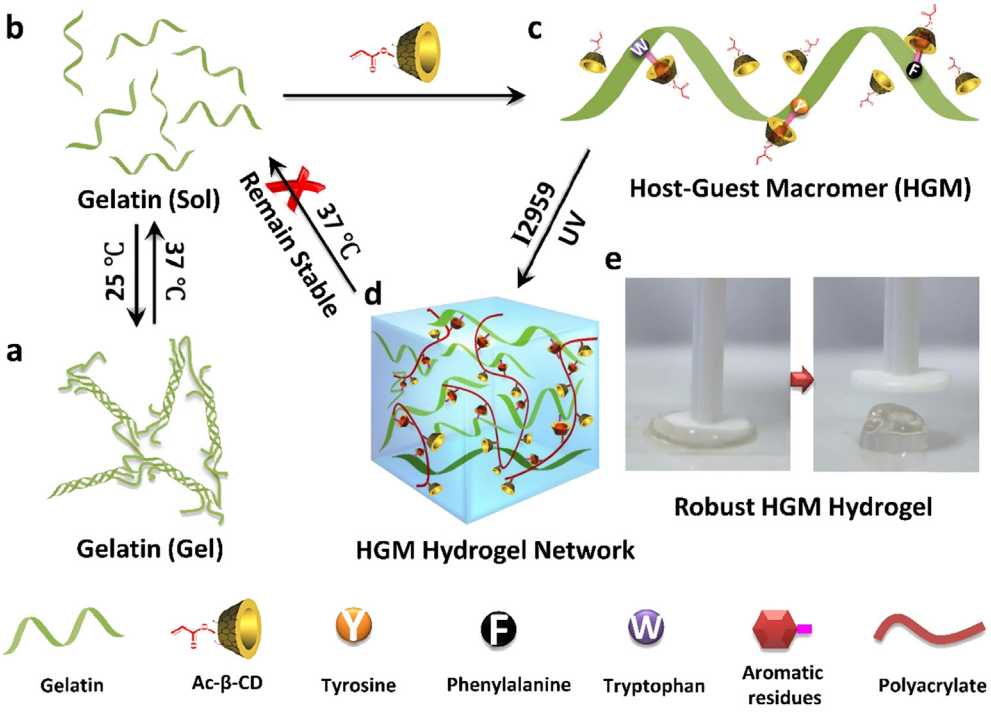

Fig. 1. (a) Solutions of pure gelatin form hydrogels below 30 °C. (b) The gelatin hydrogels dissolve at 37 °C. (c) Complexation between the free diffusing monofunctional Ac-β-CDs (with one single acrylate group per β-CD) and the aromatic residues of gelatin leads to the formation of host-guest macromere (HGM). (d) UV-initiated radical polymerization of the acrylate groups in the gelatin HGM leads to the formation of the HGM supramolecular hydrogels, which are stable at 37 °C. (e) Excellent compressibility: the HGM hydrogels can withstand cyclic excessive compression.

were used. For every SD rat, two 5 mm diameter craniotomy defects were created in the parietal bones of the skull on each side of the sagittal suture line. Dex-loaded HGM and MeGel Hydrogels without hMSCs (5 mm diameter × 1 mm thickness) were then implanted into the defects (n = 4 for each group), and the soft tissues were closed. Blank group received not implants and was used as the control group. SD rats were sacrificed after 10 weeks, and samples were harvested for the following μCT and histology analyses.

2.14. Micro-CT imaging

The collected rat calvarial samples were fixed in 70% ethyl alcohol for bone scanning using a high-resolution peripheral computed tomography (HR-pQCT, Scanco Medical. Brüttisellen, Switzerland) with a source voltage of 70 kV and current of 114 μA. The entire scan depth of 5 mm with a spatial resolution of 10 μm was used for animal experimental studies. In order to separate the signals of the mineralized tissue from the back ground signal, noise was removed using a low-pass Gaussian filter (sigma = 2.5, support = 2), and mineralized tissue was then defined at a threshold of 85 Hounsfield units. 3D images of the calvarias were reconstructed. Bone tissue volume fraction (Bone volume/Total volume, BV/TV) were measured using the built-in software of HR-pQCT system.

2.15. Gene expression analysis

Samples were homogenized in Trizol Reagent and then RNA was extracted according to the manufacturer's instructions. The RNA concentration was determined by using an ND-1000 spectrophotometer (Nanodrop Technologies). 100 ng RNA from each sample was reverse transcribed into cDNA using RevertAid First Strand cDNA Synthesis Kit from Thermo following the manufacture's protocol. Polymerase chain reaction (PCR) was operated on an Applied Biosystems 7300 Real Time PRC system using Taqman primers and probes specific for GAPDH (housekeeping gene) and other osteogenic marker gene. The relative gene expression was calculated using the $\Delta\Delta C_T$ method, where fold difference was calculated using the expression $2^{-\Delta\Delta CT}$. Each sample was internally normalized to GAPDH, and every group was compared to the expression levels of MeGel hydrogel, the quantitative value of which is determined to 1.

2.16. Biochemical analysis

One-half of each collected hydrogel (2 samples for each group, 3D *in vitro*) was divided into 2 pieces to immerse into 100 μL 1 M HCl overnight, and then neutralize the mixed solution with 5 M NaOH. The BCA and calcium content of each sample were measured by following the kits' instruction, respectively. Then the calcium content was normalized by BCA content.

2.17. Histological analysis

Samples were fixed in 4% paraformaldehyde for 24 h, embedded in paraffin, and processed using standard histological procedures. The histological sections (8 μm thick) were stained for targets of interest. Hematoxylin and eosin stain (H&E stain) and mason's trichrome stain were prepared following the manufacturers' instructions, respectively. For the type I collagen (Col I), osteocalcin (OCN), CD68, and CD163 immunochemical staining, the sections were stained using the Vectastain ABC kit and the DAB Substrate Kit for peroxidase. Briefly, sections were predigested in 0.5 mg/mL hyaluronidase for 30 min at 37 °C and incubated in 0.5 N acetic acid for 4 h at 4 °C to swell the samples prior to overnight incubation with primary antibodies, mouse monoclonal anti-collagen type I

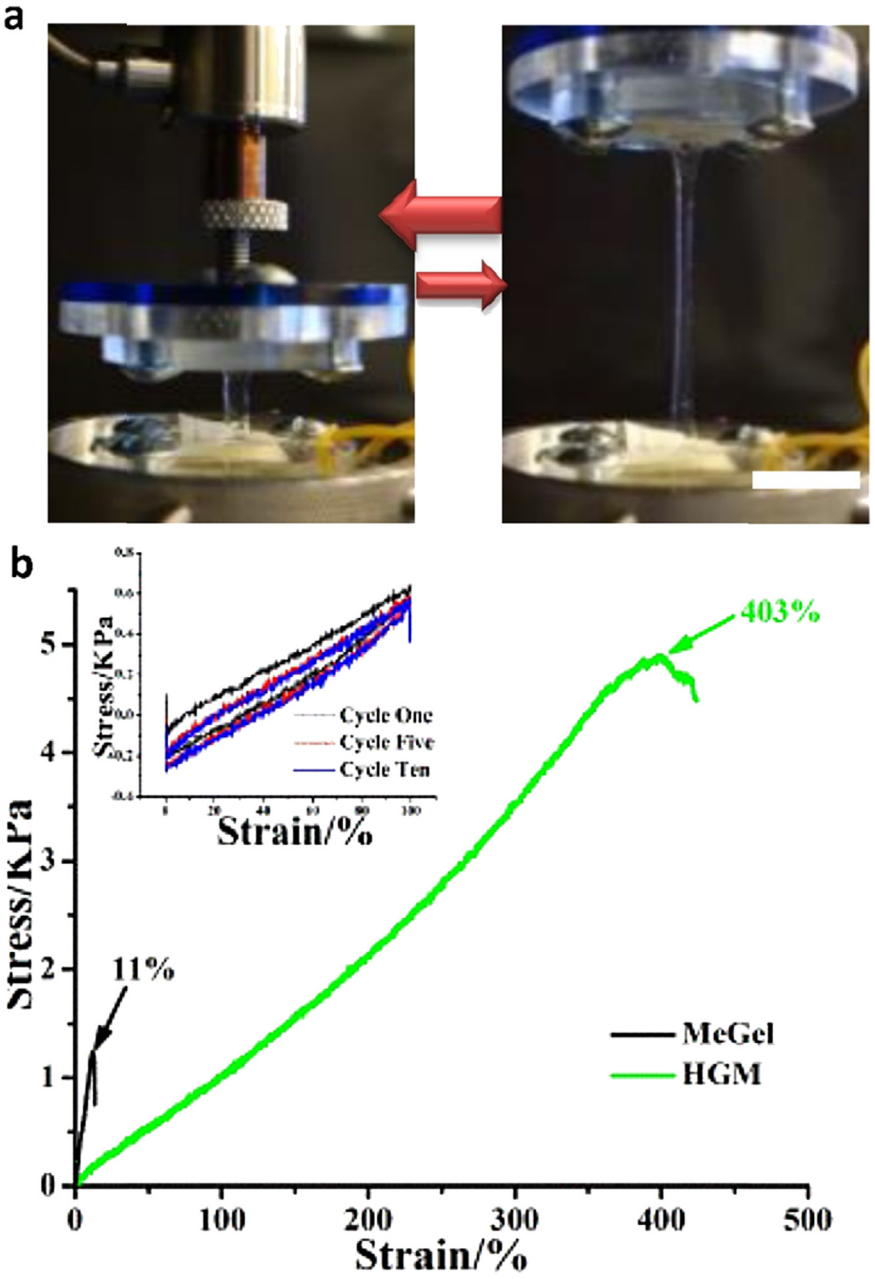

Fig. 2. (a) Superior stretchability: the HGM hydrogel can reach four times of its original length. (b) Stress vs. strain curves of MeGel and HGM hydrogels (insert: Cyclic tensile testing of HGM hydrogels at 37 °C). Scale bar: 1 cm (a).

(Takara), at dilutions of 1:200. Non-immune controls underwent the sample procedure without primary antibody incubation.

2.18. Statistical analysis

All data are presented as mean + standard deviation. Statistical analysis was performed by using two-way ANOVA and Tukey's HSD post hoc testing.

3. Results and discussion

3.1. Fabrication of supramolecular HGM hydrogels

To prepare the supramolecular gelatin host-guest macromers, we synthesize acrylated β-cyclodextrin (Ac-β-CD, average degree of acrylate substitution DS = 1, Fig. S1) [38]. By simply dissolving the gelatin polymer and Ac-β-CD in the same PBS buffer (pH7.4) at 37 °C, the gelatin host-guest macromers are readily formed driven by the host-guest inclusion complexation between the aromatic residues of gelatin (tyrosine, tryptophan, and phenylalanine) and Ac-β-CDs (Fig. 1c) [39–42]. Such molecular self-assembly is verified by 2D NOSEY NMR (Fig. S2a). It is noteworthy that the binding constant between such aromatic residues and β-CDs is relatively low (Ka~10^2 M^{-1}) [43,44]. Therefore, an excess amount of Ac-β-CDs is mixed with the gelatin to ensure more than 85% of the aromatic residues being complexed with Ac-β-CDs based on theoretical calculation (Fig. S2b) [45]. Subsequent UV initiated polymerization of the Ac-β-CDs results in the formation of HGM hydrogels that are stable at 37 °C and mechanically robust (Fig. 1d). Unlike native gelatin hydrogels which can be easily dissolved above 30 °C

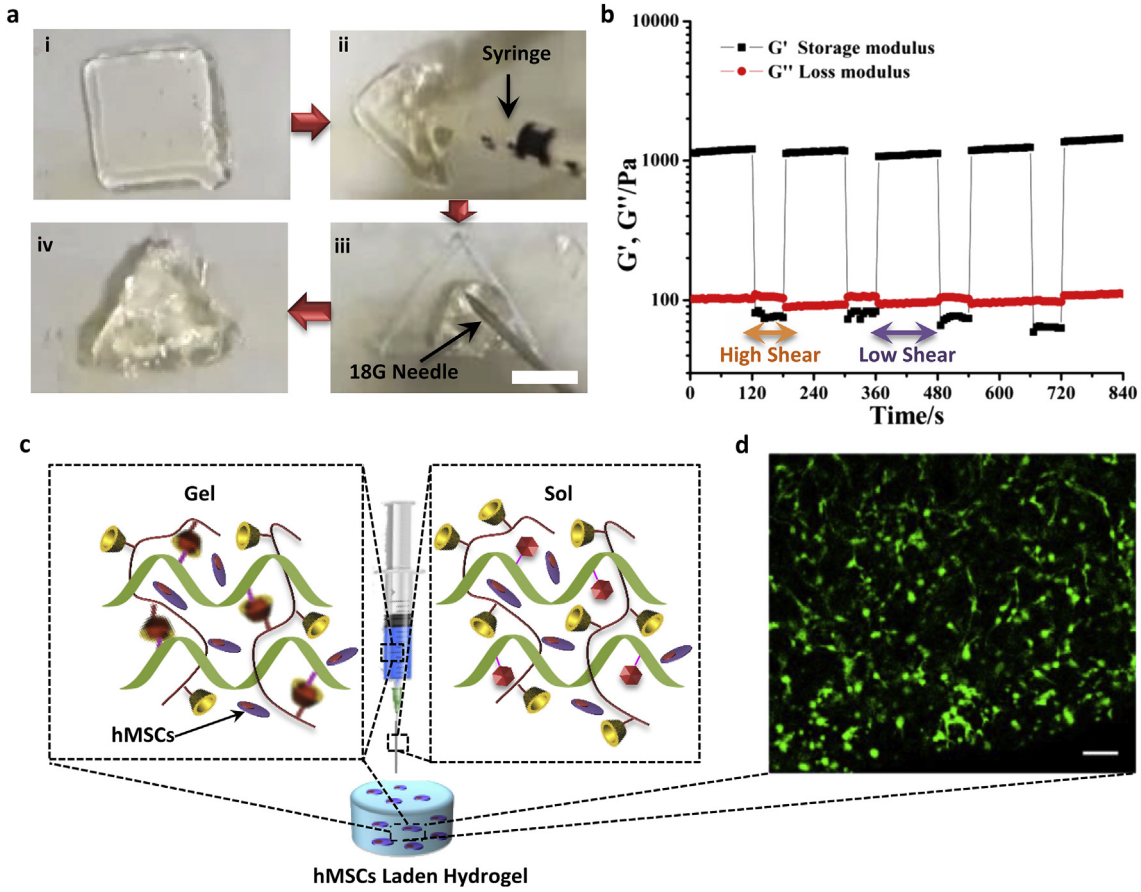

Fig. 3. (a) Moldability and injectability of the HGM hydrogels at 37 °C: i) a square-shaped hydrogel before injection; ii) the hydrogel is sucked into a syringe; iii) the hydrogel is injected into a triangular mold through a G18 needle; iv) the mold is removed after 5 min and the hydrogel adopts the shape of the mold. (b) The supramolecular hydrogels exhibit sol-gel transition during the switching of high and low shear strain as evidenced by the rheology study at 37 °C. (c) The schematic illustration of the injection of hMSC-laden HGM hydrogels: the shear stress of the injection coverts the solid HGM hydrogel into the "sol" state at 37 °C. (d) Cell viability staining of the hMSC-laden HGM hydrogels after 3 days of *in vitro* culture following the injection of the HGM hydrogels. Scale bar: 1 cm (a), 100 μm (d).

(Fig. 1b), our HGM hydrogels are stable at 37 °C and are highly compressible (Fig. 1d, and e, Video 1), indicating the robustness of the inter-gelatin host-guest crosslinking. In contrast, it has been reported that the β-CD-grafted gelatin can only form a viscous solution rather than stable hydrogels above 30 °C [39]. Such ineffective hydrogel formation are likely attributed to the inefficient host-gust interaction due to the unfavorable entropy of binding between the aromatic residuals and β-CD when they are both fixed on the bulky polymer backbones [46]. The remarkable thermostability and mechanical robustness of our HGM hydrogels (Gel_xCD_y, prepared with x% *(w/v)* gelatin, y% *(w/v)* Ac-β-CD) can be attributed to the efficient host-guest complexation during the pre-assembly between the gelatin polymers and free diffusing Ac-β-CD [7]. At 37 °C, compared to the native gelatin (Gel_8CD_0) which is a viscous solution with higher loss modulus than the storage modulus, the gelatin HGM (Gel_8CD_4 and Gel_8CD_{10}) form hydrogels upon polymerization as evidenced by the storage modulus being higher than the loss modulus (Fig. S3b). Control experiments show that mixing Ac-β-CDs solutions that are pre-treated with the same polymerizing agents as above (photoinitiator and UV exposure) with gelatin solutions results in no hydrogel formation at 37 °C (Fig. S4). Such phenomenon confirms that the pre-assembly procedure is essentially important for the preparation of robust gelatin HGM hydrogels. Furthermore, the HGM hydrogels are responsive to competitive guests as demonstrated by the disintegration of the HGM hydrogels in 1-adamantanamine hydrochloride (ADA) containing PBS (at 37 °C), indicating that the HGM hydrogels are solely crosslinked by the host-guest interactions at 37 °C (Fig. S5).

Supplementary video related to this article can be found at http://dx.doi.org/10.1016/j.biomaterials.2016.05.043.

3.2. Mechanical robustness of supramolecular HGM hydrogels

Compared to most of the biopolymer-based host-guest supramolecular hydrogels which are usually too soft to be freestanding [47,48], our gelatin HGM hydrogels show greatly improved mechanical properties. They are freestanding, elastic, and able to withstand large deformations. The tensile testing reveals that our HGM hydrogels (Gel_8CD_{10} is used hereafter unless otherwise specified) have a failure strain above 400% (Fig. 2a and b, Video 2), nearly 40 times that of the MeGel hydrogels (prepared by photopolymerization of the methacrylated gelatin, SD = 50%, 8% *(w/v)*, Fig. 2b, Fig. S6). Moreover, the HGM hydrogels are fatigue resistant under repeated tensile loading-unloading cycles as demonstrated by the nearly identical loading-unloading stress-strain curves throughout ten cycles of tensile testing (Fig. 2b insert). The mechanical resilience of the HGM hydrogels is critical to the maintenance of the hydrogel integrity after implantation in load-bearing locations such as the hip and knee joints.

Supplementary video related to this article can be found at http://dx.doi.org/10.1016/j.biomaterials.2016.05.043.

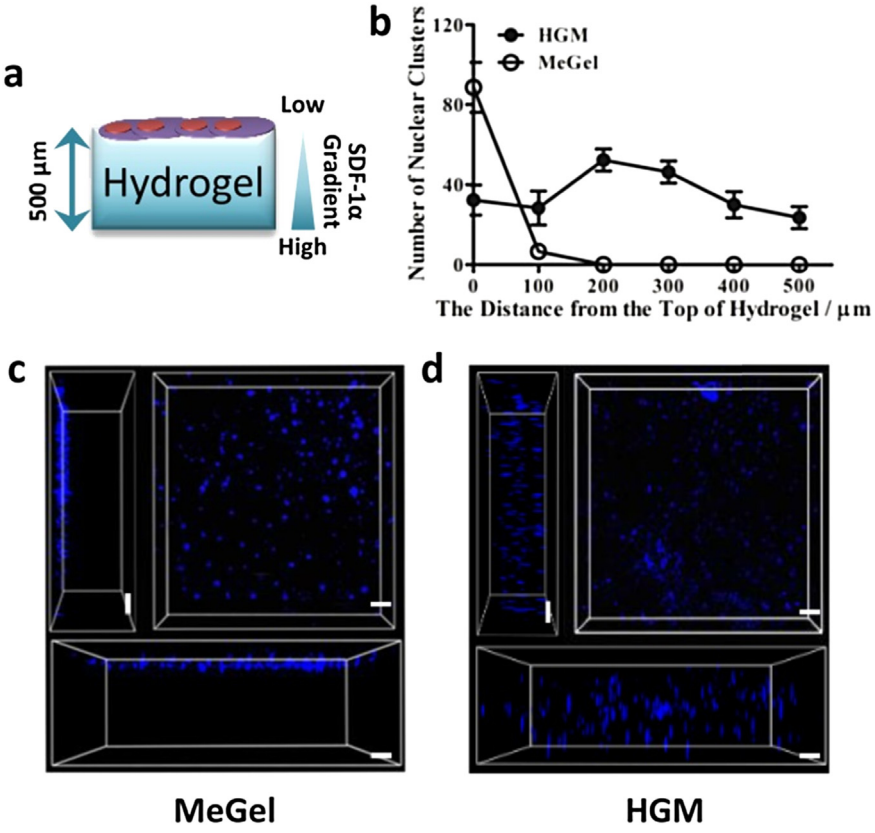

Fig. 4. (a) Schematic illustration of cell migration experiment at 37 °C. The hMSCs seeded on the surface of the HGM hydrogels infiltrate into the hydrogels, but few seeded cells infiltrate into the MeGel hydrogels. (b) The 3D distribution of DAPI-stained hMSC nuclei clusters within the MeGel and HGM hydrogels. The confocal micrographs show the 3D distribution of DAPI-stained hMSC nuclei clusters within the MeGel hydrogels (c) and HGM hydrogels (d) (right, top and front views) after 2 h of exposure to a chemoattractant gradient at 37 °C. Scale bar: 100 μm (c, d).

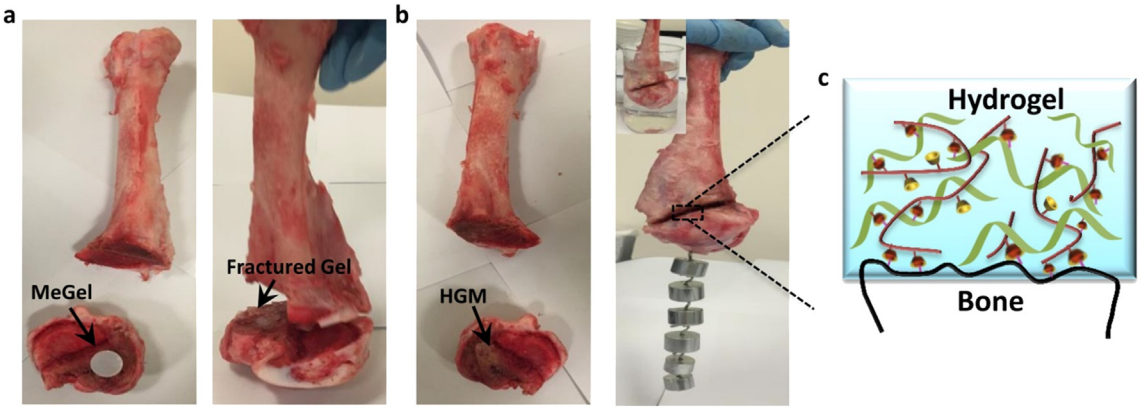

Fig. 5. (a) MeGel hydrogels fail to glue two pieces of swine bone together at 37 °C. (b) HGM hydrogels are capable of gluing the bone together: a HGM hydrogel (volume: ~1500 μl) is inserted between two pieces of swine femoral bone, and the HGM hydrogel keep the bone pieces glued together at 37 °C even after the addition of an extra 100 g of weights to the lower bone piece (inset: the HGM hydrogels bond two pieces of bone tightly even in the aqueous environment (in 37 °C PBS)). (c) The adhesion between the HGM hydrogels and the bone is likely partially mediated through the complexation between the free β-CD of HGM hydrogels and the native collagenous aromatic residues of bone. Note: the swine bone was freshly isolated from meat products acquired from a local slaughterhouse without any additional processing before being used in the adhesion test.

3.3. Dynamic properties of supramolecular HGM hydrogels based on reversible host-guest complexation

Along with the resilient and elastic mechanical properties, our HGM hydrogels are also self-healable (Fig. S8a) and re-moldable (Fig. 3a) due to the reversible host-guest interactions. They can be drawn into a syringe and injected through a G18 needle into a mold with a different shape. The injected HGM hydrogels can easily conform to the new shape of the mold and retain the shape after removal of the mold (Fig. 3a and Video 3). Moreover, the injection and remolding of the HGM hydrogels has little effect on their resilient mechanical property (Fig. S8b). Such facile injection molding of the HGM hydrogels is enabled by the reversible "sol-gel" transition during injection. The rheology analysis reveals such "sol-

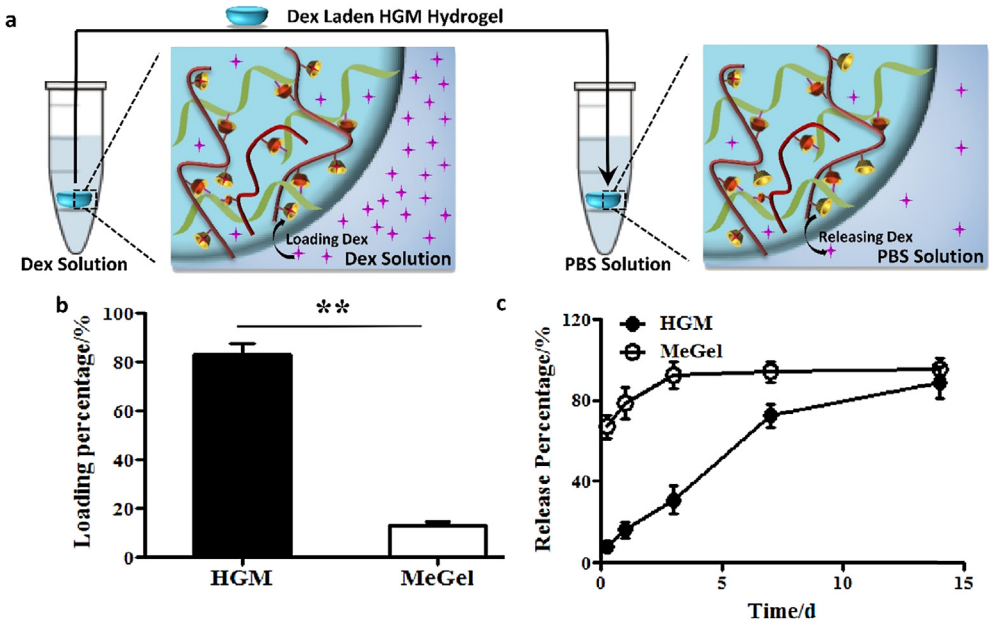

Fig. 6. (a) Schematic illustration of the sequestration and then releasing of Dex by the excess β-CDs in HGM hydrogels at 37 °C. (b) The amount of Dex absorbed into the hydrogels after incubating the hydrogels in Dex solution for 24 h at 37 °C. (c) Kinetics of Dex release from the hydrogels loaded with Dex at 37 °C.Scale bar: **$p < 0.001$.

gel" transition (Fig. 3b) under alternating high/low shear strain. The HGM hydrogels switch to the "sol" state (G" > G′) under a high shear strain of around 1000% and recover to the "gel" state (G′ > G″) under a subsequent low strain of 1%. Furthermore, we try to inject our hMSCs laden supramolceular hydrogels through a needle (Fig. 3c). Fig. 3d demonstrate that the encapsulated cells in the injected HGM hydrogels remain largely viable and are able to interact with the surrounding hydrogel matrix as evidenced by their spreading within the HGM hydrogels after the injection (viability > 95%).

Supplementary video related to this article can be found at http://dx.doi.org/10.1016/j.biomaterials.2016.05.043.

Moreover, the reversible nature of the host-guest crosslinks enables the HGM hydrogels to support cell infiltration and migration, which is important for implant biomaterials. The mobilization of the host endogenous cells including progenitor cells and stem cells is crucial to expediting the healing of tissue injuries [49–51]. The implant biomaterials that favor cell infiltration and migration will greatly facilitate the recruitment of these endogenous cells to participate in the healing process. Our cell migration assay (Fig. 4a) shows that the hMSCs seeded on the surface of MeGel hydrogels remain largely on top of the hydrogels with few cell infiltrations into the hydrogels within 200 μm from the top of hydrogels (Fig. 4b) after 2 h of exposure to a chemoattractant gradient (Fig. 4c). In contrast, nearly all the hMSCs on our HGM hydrogels penetrate into the hydrogels and migrate by large distances within the hydrogels under the same condition (Fig. 4b, d).

3.4. Tissue adhesion and drug delivery of supramolecular HGM hydrogels based on excessive Ac-β-CDs

The use of excess Ac-β-CDs not only enables the efficient formation of HGMs but also gives rise to some useful supramolecular properties of the HGM hydrogels such as bioadhesiveness and hydrophobic drug delivery. To evaluate the bioadhesiveness of the hydrogels, we use the MeGel and HGM hydrogels to glue two pieces of swine bone. Compared to MeGel hydrogels (Fig. 5a), the HGM hydrogels bond the two pieces of bone tightly even after the addition of an extra 100 g of weights to the lower bone piece at 37 °C (Fig. 5b). Based on the weight of the lower bone piece (60 g) the additional weights (100 g) and the adhesion area of the hydrogel (176.625 mm^2), the average adhesive stress between the bone and HGM hydrogel is estimated to be 8.88 kPa. Furthermore, the HGM hydrogels maintain the adhesion to bone even under an aqueous condition (in PBS, Fig. 5b inset). Furthermore, the lap-shear test also demonstrates that our HGM hydrogels has much better adhesive property than the MeGel hdyrogels (Fig. S10). Considering the highly hydrated polymeric structure and the absence of reactive bonding groups in the HGM hydrogels, the bioadhesive property of the HGM hydrogels is remarkable. The complexation between the β-CDs in the HGM hydrogels and the native collagenous aromatic residues together with potential hydrogen bonding between the hydrogel structures and tissue matrix components may have contributed to the bioadhesive property of the HGM hydrogels, which is important for the retention of the hydrogels in the intended location after implantation (Fig. 5c). Furthermore, swelling test shows that the HGM hydrogels have a higher swelling ratio compared to the MeGel hydrogels (Fig. S9), indicating that the HGM hydrogels remain adhesive under a highly swollen state.

Moreover, since cyclodextrins have long been used in the pharmaceutical industry to improve the solubility and bioavailability of hydrophobic drugs [44,52], our HGM hydrogels can hold hydrophobic small molecular drugs, such as Dexamethasone (Dex) in the unoccupied hydrophobic β-CD cavities (Fig. 6a). After soaking in Dex solution, the HGM hydrogels absorb as much as about 80% of the total Dex in the solution, which is much higher than that absorbed by the MeGel hydrogels (Fig. 6b). In the following drug release test, the HGM hydrogels release Dex continuously for up to 14 days at an almost constant rate (Fig. 6c).

3.5. Enhanced differentiation of hMSCs in supramolecular HGM hydrogels

We then evaluate the osteogenesis of the hMSCs in our HGM hydrogels *in vitro* and *in vivo*. After 14 days of culture in osteogenic

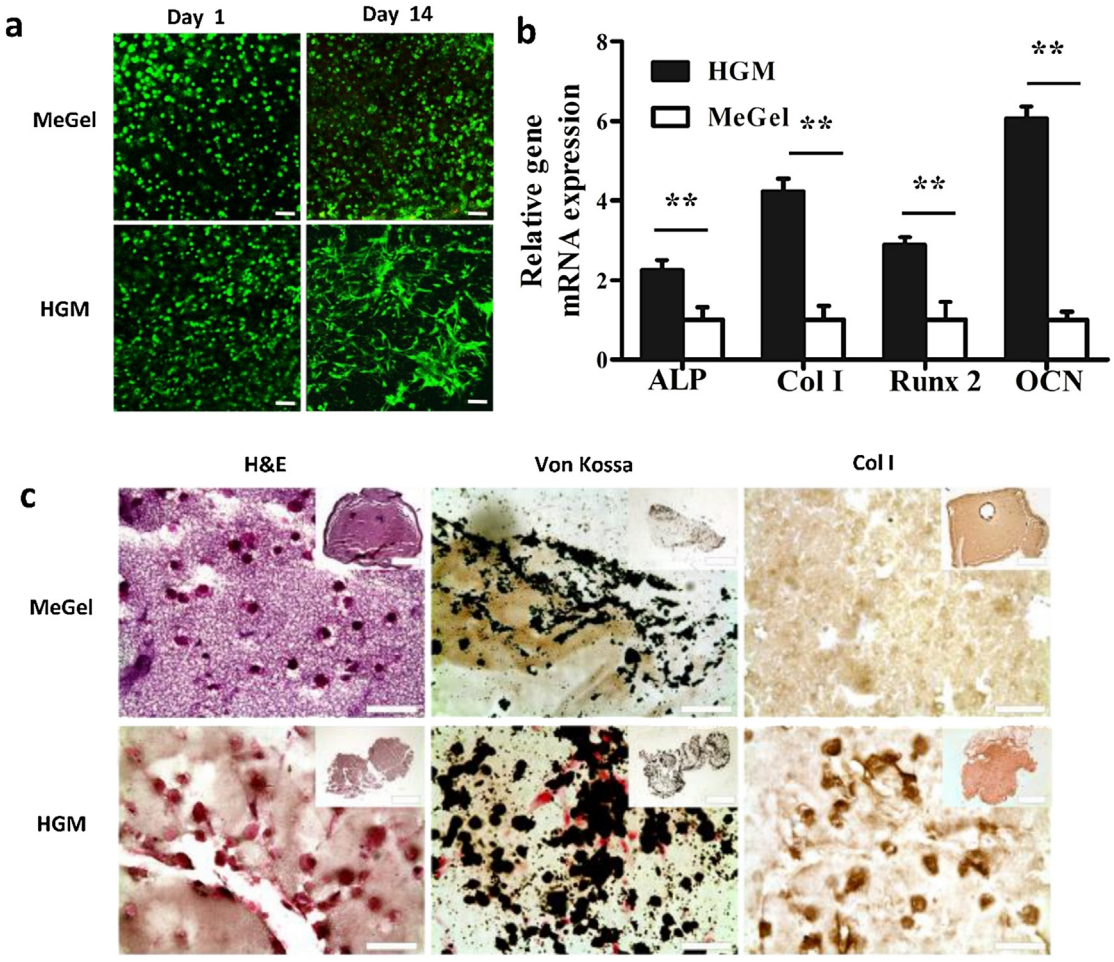

Fig. 7. (a) Cell viability staining of the hMSC-laden MeGel and HGM hydrogels after 1 day (left) and 14 days (right) of culture. (b) Gene expression (normalized to GAPDH) of selected osteogenic markers (alkaline phosphatase (ALP), type I collagen (Col I), runt-related transcription factor 2 (Runx2), and osteocalcin (OCN)). (c) Hematoxylin and eosin stain (H&E) staining, von kossa staining, and type I collagen (Col I) immunohistochemical staining of the hMSC-laden HGM and MeGel hydrogels after 14 days of osteogenic culture. Scale bars: 100 mm (a), 50 mm (c, and 100 mm (insert)). **$p < 0.001$.

media, the majority (>95%) of the hMSCs encapsulated in the HGM hydrogels remain viable (Fig. 7a). Strikingly, the hMSCs encapsulated in the HGM hydrogels adopt a stellate morphology after 14 days of culture, whereas the hMSCs in the MeGel hydrogels remain in the initial rounded morphology (Fig. 7a). This finding confirms our hypothesis that the cells encapsulated in the HGM hydrogels are able to actively interact with the surrounding hydrogel structures, likely by cell traction forces, due to the reversible crosslinking in the HGM hydrogels. Moreover, the hMSCs in the HGM hydrogels exhibit significantly higher expression of osteogenic marker genes including Runx2, type I collagen, ALP and osteocalcin compared to those in the MeGel hydrogels that have the same gelatin content as that of the HGM hydrogels (Fig. 7b). Consistent with the gene expression data, the calcium and the type I collagen content, two important markers for osteogenesis, are also higher in the HGM hydrogels than in the MeGel hydrogels (Fig. 7c and Fig. S12). As described above, the HGM hydrogels favor cell spreading, and therefore the development of the cell cytoskeletal tension, which has been shown to promote osteogenesis of hMSCs [53,54].

The hMSCs seeded in the HGM gelatin hydrogels, which are loaded with a bolus dose of Dex during hydrogel fabrication and cultured in Dex-free media (HGM-Dex in Hydrogel), show similar expression level of the osteogenic marker genes as those in the HGM hydrogels cultured with fresh Dex supplementation after each media change (HGM-Dex in Media) (Fig. S13). Both these two groups have significantly higher osteogenic gene expressions than the hMSC-laden MeGel hydrogels receiving continuous Dex supplementation (Fig. S13). This finding demonstrates the efficacy of our HGM hydrogels as the potential carrier material for the delivery of stem cells together with the differentiation-inducing drugs to tissue defects *in vivo*, where continuous addition of drugs is usually impractical.

3.6. Bone regeneration in acellular supramolecular HGM hydrogels

We further evaluated the efficacy of our HGM hydrogels for bone regeneration in a rat calvarial bone defect model. The implanted acellular Dex-laden HGM hydrogels support more mineralized tissue deposition in the defects compared to the Dex-laden MeGel hydrogels (Fig. 8a and Fig, S14). The histological staining results show that the defects of the blank control group are filled with a thin layer of loose connective tissue with no staining against osteocalcin, a key bone marker (Fig. S15). Consistent with prior results from the nude mice study (Fig. S16), a large number of cells migrate into the implanted HGM hydrogels, while there are no cells found in the MeGel hydrogels (Fig. 8a). The histological sections of the HGM hydrogels show more intense staining against type I collagen compared to those of the MeGel hydrogels (Fig. 8a).

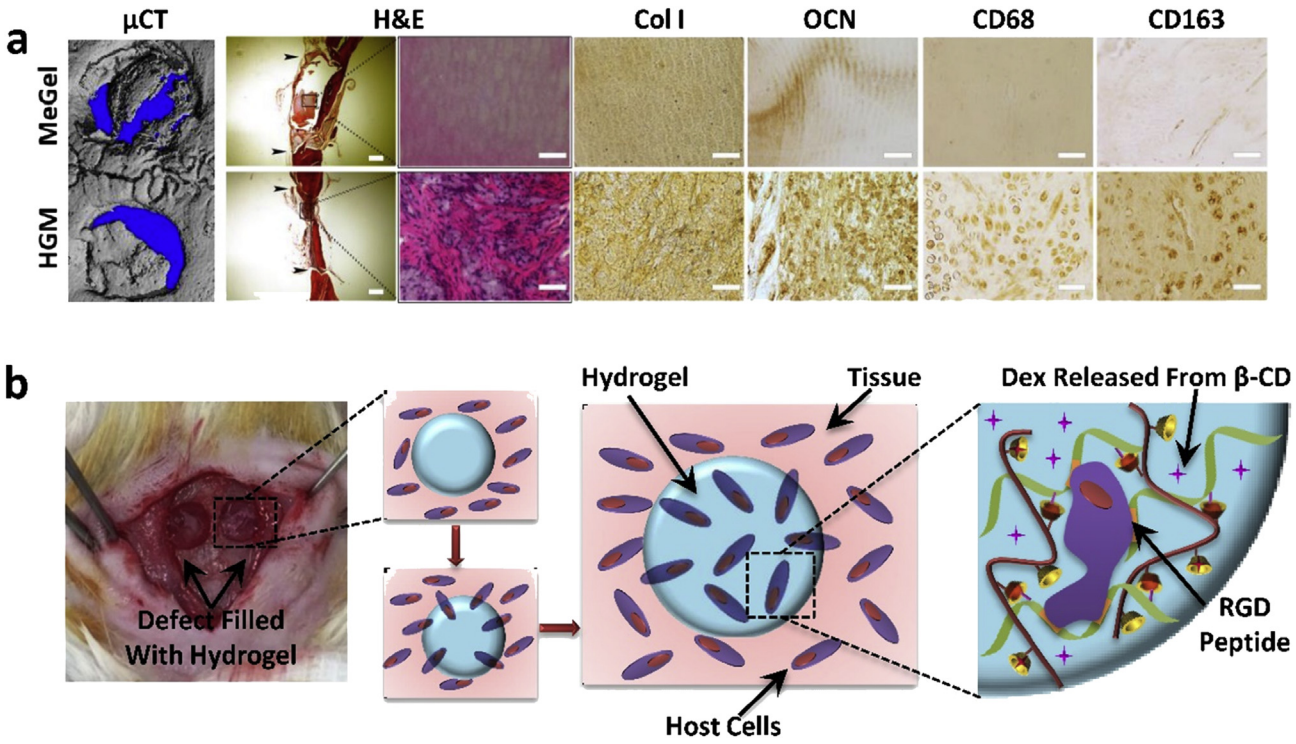

Fig. 8. (a) Representative μCT reconstitution, H&E staining, type I collagen (Col I), osteocalcin (OCN), CD68, and CD163 immunohistochemical staining of the Dex-laden MeGel and HGM hydrogels after ten weeks of implantation in rat calvarial bone defects (black narrow: the defect boundary). (b) Dex-laden HGM hydrogels facilitate the infiltration and migration of the host cells. The HGM hydrogels also can sustain the protracted release Dex, which is important to the bone regeneration *in situ*. Scale bars: 100 μm (a), 50 μm (c, and 100 μm (inserts), 50 μm (e, except the leftmost column of H&E staining, 500 μm). $^{**}p < 0.001$.

Furthermore, the osteocalcin expression is detected in many cells in the HGM hydrogels, thus indicating the migration of endogenous osteoblastic cells into the implanted HGM hydrogels (Fig. 8a). Moreover, the immunohistochemical staining against CD68 and CD163, markers of M1 and M2 macrophage, respectively, are also only found in the implanted HGM hydrogels but not in the MeGel hydrogels (Fig. 8a). The coordination between the early inflammation initiated by the M1 macrophages and the subsequent appearance of the anti-inflammatory M2 macrophages are believed to be essential to tissue healing and regeneration [55,56]. A previous study specifically shows that macrophages can induce osteogenic differentiation of hMSCs and enhance matrix mineralization [57]. Therefore, this experiment demonstrates that our HGM hydrogels have the potential to modulate macrophage polarization and support *in situ* tissue regeneration without using exogenous cells, thereby greatly simplifying the regenerative therapy and avoiding the potential lengthy regulatory approval process (Fig. 8b).

4. Discussion

This study demonstrates that our novel and convenient "Host-Guest Macromer" (HGM) approach produces supramolecular hydrogels of desirable attributes that are critical to their successful application in regenerative medicine. Unlike most of the traditional supramolecular hydrogels that are weak in mechanical properties, our HGM hydrogels are mechanically robust and are therefore suitable for implantation to the surgical sites of loading bearing nature.

Furthermore, our HGM hydrogels are injectable in the gelation state, capable of self-healing. Compared to conventional injectable hydrogels that generally require the preparation of the precursor solutions and immediate injection to form the hydrogels *in situ* via either chemical crosslinking or physical interactions (e.g. thermo-responsive hydrogels) [2], our HGM hydrogels can be pre-formed with the encapsulated therapeutic cells and drugs first, maintained in the culture condition, and injected into the recipients in the gelation form at a prescribed time later. It will offer great convenience to the potential surgical users and expedite the clinical operations significantly. Furthermore, the HGM hydrogels regain the "gel" state and conform to the geometry of the injection sites immediately after exiting from the needle tip. It limits the potential loss of the injected materials due to spreading and leakage into unintended locations neighboring the injection sites, thereby enhancing the targeted delivery of the carried therapeutic cargos.

Our cell migration analysis shows that our HGM hydrogels better support cell infiltration and migration than the conventional chemically crosslinking MeGel hydrogels. Previous studies have shown that stiffer hydrogels promote cell migrations compared to softer hydrogels of the same material [54,55]. Therefore, the enhanced cell migrations within our HGM hydrogels, which are softer than the MeGel hydrogels, are likely due to the reversible nature of the host-guest complexation crosslinks in the supramolecular hydrogels. We speculate that the weak host-guest interaction between the aromatic residues of gelatin and β-cyclodextrin, which is the sole crosslinking mechanism in our supramolecular hydrogels, allows infiltration of the cells into the hydrogels. We postulate that hMSCs are capable of "breaking" the weak physical crosslinks in the HGM hydrogels via cell traction forces to find a way for migration. After the passage of the cells, the disconnected host and guest molecules in the HGM hydrogels bind to each other again. Therefore, the HGM hydrogels facilitate cell infiltration and migration without suffering structural damage. Meanwhile, a separate unpublished study in our group shows that cells fail to infiltrate into the supramolecular hydrogels that are crosslinked by

the host-guest complexation of the β-cyclodextrin and adamantane, which has much higher binding affinity than that of the complexation between β-cyclodextrin and aromatic groups. This may indicate that the cell traction force may be only sufficient to open up the weak but not strong host-guest complexation, and careful selection of the host-guest pairs may be critical to the design of host-guest hydrogels that permit cell infiltration and migration. This property helps our HGM hydrogels take the host endogenous cells including progenitor cells and stem cells to promote the *in situ* tissue regeneration.

Moreover, the spare unoccupied β-CD cavities in the HGM hydrogels can potential complex with the aromatic residues of the native collagens to help the HGM hydrogels adhere to the native tissues. This bioadhesive property of our hydrogels can potentially improve the retention of the implanted hydrogels in the intended location, and this can reduce the off target effects due to the unwanted movement of the implants. The excess unoccupied β-CD cavities in the HGM hydrogels also help to hold hydrophobic small molecular drugs, such as Dex and modulate the release of the drugs. These results demonstrate the enhanced storage and sustained release of the hydrophobic drugs by our HGM hydrogels, which is essential to promoting stem cell differentiations post implantation and tissue regeneration. Under *in vitro* culture, the HGM hydrogels significantly enhance the osteogenic differentiation of the encapsulated hMSCs compared to the chemically crosslinked MeGel hydrogels. For *in vivo* experiment, the acellular HGM hydrogels implanted in rat calvarial bone defects can recruit endogenous osteoblastic cells and regulate the polarization of the attracted macrophages, leading to enhanced tissue deposition in the defect. In contrast, minimal cells and tissue elaboration can be found in the implanted MeGel hydrogels. The HGM hydrogels show the great potential to support *in situ* tissue regeneration by mobilizing the endogenous cells. Therefore, this acellular approach not only potentially simplifies the regulatory approval process of the regenerative therapy by eliminating the use of exogenous cell but also lowers the risk associated with these cells.

5. Conclusion

Collectively, the present work demonstrates an effective "Host-Guest Macromer" approach for the facile preparation of supramolecular HGM gelatin hydrogels for potential applications in regenerative medicine. Such HGM hydrogels combine different desirable properties and can fulfill the multifold requirements of applications in regenerative medicine. The HGM hydrogels are mechanically robust as highly deformable and resilient freestanding constructs due to the efficient host-guest complexation, making them suitable biomaterials for repairing load bearing tissues. Meanwhile, the HGM hydrogels are self-healable, injectable and re-moldable due to the reversible nature of the host-guest interactions, thus facilitating the easy surgical usage via the straightforward injection molding. The HGM hydrogels are also bio-adhesive and are able to retain and release hydrophobic drugs, thereby enabling the delivery and long-term release of drugs the targeted locations. Furthermore, our HGM supramolecular hydrogels aid cell infiltration and migration and support stem cell differentiation and *in situ* tissue regeneration, making them ideal biomaterial carrier of therapeutic cells and drugs to assist the repair and regeneration of injured tissues such as bone, cartilage, and tendon.

Acknowledgements

The work described in this paper is supported by a General Research Fund grant from the Research Grants Council of Hong Kong (Project No. 14202215). This research is also supported by project BME-p3-15 of the Shun Hing Institute of Advanced Engineering, The Chinese University of Hongkong, The Chinese University of Hong Kong. This work is supported by the Health and Medical Research Fund, the Food and Health Bureau, the Government of the Hong Kong Special Administrative Region (reference no.: 02133356). Project 31570979 is supported by the National Natural Science Foundation of China. This research is supported by the Chow Yuk Ho Technology Centre for Innovative Medicine, The Chinese University of Hong Kong.

Appendix A. Supplementary data

Supplementary data related to this article can be found at http://dx.doi.org/10.1016/j.biomaterials.2016.05.043.

References

[1] D. Seliktar, Designing cell-compatible hydrogels for biomedical applications, Science 336 (6085) (2012) 1124–1128.
[2] J. Thiele, Y. Ma, S. Bruekers, et al., 25th Anniversary article: designer hydrogels for cell cultures: a materials selection guide, Adv. Mater. 26 (1) (2014) 125–148.
[3] J. Lam, E.C. Clark, E.L.S. Fong, et al., Evaluation of cell-laden polyelectrolyte hydrogels incorporating poly (L-Lysine) for applications in cartilage tissue engineering, Biomaterials 83 (2016) 332–346.
[4] J.A. Burdick, G.D. Prestwich, Hyaluronic acid hydrogels for biomedical applications, Adv. Mater. 23 (12) (2011) H41–H56.
[5] B. Balakrishnan, R. Banerjee, Biopolymer-based hydrogels for cartilage tissue engineering, Chem. Rev. 111 (8) (2011) 4453–4474.
[6] A. Harada, R. Kobayashi, Y. Takashima, et al., Macroscopic self-assembly through molecular recognition, Nat. Chem. 3 (1) (2011) 34–37.
[7] T. Kakuta, Y. Takashima, M. Nakahata, et al., Preorganized hydrogel: self-healing properties of supramolecular hydrogels formed by polymerization of host–guest-monomers that contain cyclodextrins and hydrophobic guest groups, Adv. Mater. 25 (20) (2013) 2849–2853.
[8] L.S.M. Teixeira, J. Feijen, C.A. van Blitterswijk, et al., Enzyme-catalyzed crosslinkable hydrogels: emerging strategies for tissue engineering, Biomaterials 33 (5) (2012) 1281–1290.
[9] Y.H. Kim, H. Furuya, Y. Tabata, Enhancement of bone regeneration by dual release of a macrophage recruitment agent and platelet-rich plasma from gelatin hydrogels, Biomaterials 35 (1) (2014) 214–224.
[10] M. Zhu, S. Lin, Y. Sun, et al., Hydrogels functionalized with N-cadherin mimetic peptide enhance osteogenesis of hMSCs by emulating the osteogenic niche, Biomaterials 77 (2016) 44–52.
[11] Y.C. Toh, J. Xing, H. Yu, Modulation of integrin and E-cadherin-mediated adhesions to spatially control heterogeneity in human pluripotent stem cell differentiation, Biomaterials 50 (2015) 87–97.
[12] A.T. Neffe, B.F. Pierce, G. Tronci, et al., One step creation of multifunctional 3D architectured hydrogels inducing bone regeneration, Adv. Mater. 27 (10) (2015) 1738–1744.
[13] R.S. Jacob, D. Ghosh, P.K. Singh, et al., Self healing hydrogels composed of amyloid nano fibrils for cell culture and stem cell differentiation, Biomaterials 54 (2015) 97–105.
[14] K.M. Schultz, K.A. Kyburz, K.S. Anseth, Measuring dynamic cell–material interactions and remodeling during 3D human mesenchymal stem cell migration in hydrogels, Proc. Natl. Acad. Sci. 112 (29) (2015) E3757–E3764.
[15] N. Huebsch, E. Lippens, K. Lee, et al., Matrix elasticity of void-forming hydrogels controls transplanted-stem-cell-mediated bone formation, Nat. Mater. 14 (12) (2015) 1269–1277.
[16] T.T. Lee, J.R. García, J.I. Paez, et al., Light-triggered in vivo activation of adhesive peptides regulates cell adhesion, inflammation and vascularization of biomaterials, Nat. Mater. 14 (3) (2015) 352–360.
[17] E.A. Appel, J. del Barrio, X.J. Loh, et al., Supramolecular polymeric hydrogels, Chem. Soc. Rev. 41 (18) (2012) 6195–6214.
[18] C.B. Rodell, A.L. Kaminski, J.A. Burdick, Rational design of network properties in guest–host assembled and shear-thinning hyaluronic acid hydrogels, Biomacromolecules 14 (11) (2013) 4125–4134.
[19] K.M. Park, J.A. Yang, H. Jung, et al., In situ supramolecular assembly and modular modification of hyaluronic acid hydrogels for 3D cellular engineering, Acs Nano 6 (4) (2012) 2960–2968.
[20] H. Jung, J.S. Park, J. Yeom, et al., 3D tissue engineered supramolecular hydrogels for controlled chondrogenesis of human mesenchymal stem cells, Biomacromolecules 15 (3) (2014) 707–714.
[21] M. Mehdizadeh, H. Weng, D. Gyawali, et al., Injectable citrate-based mussel-inspired tissue bioadhesives with high wet strength for sutureless wound closure, Biomaterials 33 (32) (2012) 7972–7983.
[22] P.Y.W. Dankers, M.J.A. van Luyn, A. Huizinga-van der Vlag, et al., Development and in-vivo characterization of supramolecular hydrogels for intrarenal drug delivery, Biomaterials 33 (20) (2012) 5144–5155.
[23] Y. Haraguchi, T. Shimizu, T. Sasagawa, et al., Fabrication of functional three-

dimensional tissues by stacking cell sheets in vitro, Nat. Protoc. 7 (5) (2012) 850–858.
[24] S.R. Shin, B. Aghaei-Ghareh-Bolagh, T.T. Dang, et al., Cell-laden microengineered and mechanically tunable hybrid hydrogels of gelatin and graphene oxide, Adv. Mater. 25 (44) (2013) 6385–6391.
[25] R.Z. Lin, Y.C. Chen, R. Moreno-Luna, et al., Transdermal regulation of vascular network bioengineering using a photopolymerizable methacrylated gelatin hydrogel, Biomaterials 34 (28) (2013) 6785–6796.
[26] B.P. Mahadik, S.P. Haba, L.J. Skertich, et al., The use of covalently immobilized stem cell factor to selectively affect hematopoietic stem cell activity within a gelatin hydrogel, Biomaterials 67 (2015) 297–307.
[27] K. Cheng, A. Blusztajn, D. Shen, et al., Functional performance of human cardiosphere-derived cells delivered in an in situ polymerizable hyaluronan-gelatin hydrogel, Biomaterials 33 (21) (2012) 5317–5324.
[28] A. Duconseille, T. Astruc, N. Quintana, et al., Gelatin structure and composition linked to hard capsule dissolution: a review, Food Hydrocoll. 43 (2015) 360–376.
[29] Y.C. Chen, R.Z. Lin, H. Qi, et al., Functional human vascular network generated in photocrosslinkable gelatin methacrylate hydrogels, Adv. Funct. Mater. 22 (10) (2012) 2027–2039.
[30] J. Visser, D. Gawlitta, K.E.M. Benders, et al., Endochondral bone formation in gelatin methacrylamide hydrogel with embedded cartilage-derived matrix particles, Biomaterials 37 (2015) 174–182.
[31] R.Z. Lin, Y.C. Chen, R. Moreno-Luna, et al., Transdermal regulation of vascular network bioengineering using a photopolymerizable methacrylated gelatin hydrogel, Biomaterials 34 (28) (2013) 6785–6796.
[32] M. Nikkhah, N. Eshak, P. Zorlutuna, et al., Directed endothelial cell morphogenesis in micropatterned gelatin methacrylate hydrogels, Biomaterials 33 (35) (2012) 9009–9018.
[33] N.A. Peppas, Y. Huang, M. Torres-Lugo, et al., Physicochemical foundations and structural design of hydrogels in medicine and biology, Annu. Rev. Biomed. Eng. 2 (1) (2000) 9–29.
[34] M.J. Coelho, M. Femandes, Human bone cell cultures in biocompatibility testing. Part II: effect of ascorbic acid, β-glycerophosphate and dexamethasone on osteoblastic differentiation, Biomaterials 21 (11) (2000) 1095–1102.
[35] K. Johnson, S. Zhu, M.S. Tremblay, J.N. Payette, J. Wang, L.C. Bouchez, S. Meeusen, A. Althage, C.Y. Cho, X. Wu, P.G. Schultz, A stem-cell based approach to cartilage repair, Science 226 (6082) (2012) 717–721.
[36] J.C. Kaczmarek, A. Tieppo, C.J. White, M.E. Byrne, Adjusting biomaterial composition to achieve controlled multiple-day release of dexamethasone from an extended-wear silicone hydrogel contact lens. Journal of Biomaterials Science, Polym. Ed. 25 (1) (2014) 88–100.
[37] M.L. Kang, J.Y. Ko, J.E. Kim, G.I. Im, Intra-articular delivery of kartogenin-conjugated chitosan nano/microparticles for cartilage regeneration, Biomaterials 35 (37) (2014) 9984–9994.
[38] M.J. Kettel, F. Dierkes, K. Schaefer, et al., Aqueous nanogels modified with cyclodextrin, Polymer 52 (9) (2011) 1917–1924.
[39] D.B. Bernert, K. Isenbügel, H. Ritter, Synthesis of a novel glycopeptide by polymeranalogous reaction of gelatin with mono-6-para-toluenesulfonyl-β-cyclodextrin and its supramolecular properties, Macromol. Rapid Commun. 32 (4) (2011) 397–403.
[40] L. Qin, X.W. He, W.Y. Li, et al., Molecularly imprinted polymer prepared with bonded β-cyclodextrin and acrylamide on functionalized silica gel for selective recognition of tryptophan in aqueous media, J. Chromatogr. A 1187 (1) (2008) 94–102.
[41] M. Ma, S. Xu, P. Xing, et al., A multistimuli-responsive supramolecular vesicle constructed by cyclodextrins and tyrosine, Colloid Polym. Sci. 293 (3) (2015) 891–900.
[42] M. Jana, S. Bandyopadhyay, Molecular dynamics study of β-cyclodextrin–phenylalanine (1: 1) inclusion complex in aqueous medium, J. Phys. Chem. B 117 (31) (2013) 9280–9287.
[43] M.V. Rekharsky, Y. Inoue, Complexation thermodynamics of cyclodextrins, Chem. Rev. 98 (5) (1998) 1875–1918.
[44] M.E. Davis, M.E. Brewster, Cyclodextrin-based pharmaceutics: past, present and future, Nat. Rev. Drug Discov. 3 (12) (2004) 1023–1035.
[45] K. Wei, J. Li, G. Chen, et al., Dual molecular recognition leading to a protein–polymer conjugate and further self-assembly, ACS Macro Lett. 2 (3) (2013) 278–283.
[46] A. Charlot, R. Auzély-Velty, Synthesis of novel supramolecular assemblies based on hyaluronic acid derivatives bearing bivalent β-cyclodextrin and adamantane moieties, Macromolecules 40 (4) (2007) 1147–1158.
[47] E.A. Appel, R.A. Forster, M.J. Rowland, et al., The control of cargo release from physically crosslinked hydrogels by crosslink dynamics, Biomaterials 35 (37) (2014) 9897–9903.
[48] E.R. Janeček, J.R. McKee, C.S.Y. Tan, et al., Hybrid supramolecular and colloidal hydrogels that bridge multiple length scales, Angew. Chem. Int. Ed. 54 (18) (2015) 5383–5388.
[49] F.M. Chen, L.A. Wu, M. Zhang, et al., Homing of endogenous stem/progenitor cells for in situ tissue regeneration: promises, strategies, and translational perspectives, Biomaterials 32 (12) (2011) 3189–3209.
[50] J.A. Burdick, R.L. Mauck, J.H. Gorman, et al., Acellular biomaterials: an evolving alternative to cell-based therapies, Sci. Transl. Med. 5 (176) (2013) 176 ps4-176ps4.
[51] I.K. Ko, S.J. Lee, A. Atala, et al., In situ tissue regeneration through host stem cell recruitment, Exp. Mol. Med. 45 (11) (2013) e57.
[52] K. Uekama, F. Hirayama, T. Irie, Cyclodextrin drug carrier systems, Chem. Rev. 98 (5) (1998) 2045–2076.
[53] R. McBeath, D.M. Pirone, C.M. Nelson, et al., Cell shape, cytoskeletal tension, and RhoA regulate stem cell lineage commitment, Dev. Cell 6 (4) (2004) 483–495.
[54] S. Khetan, M. Guvendiren, W.R. Legant, et al., Degradation-mediated cellular traction directs stem cell fate in covalently crosslinked three-dimensional hydrogels, Nat. Mater. 12 (5) (2013) 458–465.
[55] R. Sridharan, A.R. Cameron, D.J. Kelly, et al., Biomaterial based modulation of macrophage polarization: a review and suggested design principles, Mater. Today 18 (6) (2015) 313–325.
[56] E. Aikawa, M. Nahrendorf, J.L. Figueiredo, et al., Osteogenesis associates with inflammation in early-stage atherosclerosis evaluated by molecular imaging in vivo, Circulation 116 (24) (2007) 2841–2850.
[57] P. Guihard, Y. Danger, B. Brounais, et al., Induction of osteogenesis in mesenchymal stem cells by activated monocytes/macrophages depends on oncostatin M signaling, Stem Cells 30 (4) (2012) 762–772.